PCCP

COMMUNICATION

View Article Online
View Journal

Cite this: DOI: 10.1039/d6cp00273k

Received 26th January 2026,
Accepted 3rd April 2026

DOI: 10.1039/d6cp00273k

rsc.li/pccp

Green circularly polarized luminescence with a high dissymmetry factor emitted by a [2.2]fluorenonophane

André Loleit, [a] Lars Eckhardt, [b] Markus Ströbele, [c] Jonas L. Hiller, [b] Marcus Scheele *[b] and Holger F. Bettinger *[a]

We report the chiroptical properties of enantiopure [2.2]fluorenonophane measured using electronic circular dichroism and circularly polarized luminescence spectroscopy. The target compound exhibited excellent chiroptical properties with high dissymmetry factors of $g_{abs} = \pm 1.3 \times 10^{-2}$ and $g_{lum} = +2.5 \times 10^{-2}/-2.6 \times 10^{-2}$ in a wide range of solvents, accompanied by strong indications of excimer formation. This study emphasizes the outstanding role of [2.2]paracyclophanes as model systems for small molecules with relatively large CPL and expands this compound class by using the easily accessible and modifiable fluorenone derivative.

The intriguing photophysical phenomenon of circularly polarized luminescence (CPL) is currently attracting the attention of researchers due to its potential applications in advanced technologies such as 3D displays,[1–3] chiral sensing[4–6] or information storage devices.[7–9] CPL refers to the differential emission of photons in the left and right circularly polarized states, which is usually quantified by the dissymmetry factor of luminescence: $g_{lum} = 2\Delta I(\lambda)/I(\lambda)$, where $\Delta I(\lambda) = I_L(\lambda) - I_R(\lambda)$ and $I(\lambda) = I_L(\lambda) + I_R(\lambda)$.[10] By definition, the g_{lum} values can range from −2 to +2, corresponding to fully left or right circularly polarized light, respectively. One strategy to achieve CPL is the use of non-racemic mixtures of chiral luminophores that preferentially emit in one polarization state.[11–13] Small chiral organic molecules typically display g_{lum} values in the range of 10^{-5}–10^{-3}, whereas examples with $g_{lum} > 10^{-2}$ or even 10^{-1} are only rarely reported.[11,14–18] Hence, designing and synthesizing molecules with high g_{lum} values is still a key challenge in CPL research.[19]

The favorable optoelectronic properties[20,21] combined with the prochiral nature of the [2.2]paracyclophane (PCP) scaffold make it an ideal platform for designing CPL emitters.[22–25] By substituting or extending the π system of [2.2]PCP, not only can planar chirality be induced, but the optoelectronic properties can also be adjusted. Morisaki and coworkers, who have been very active in the field of [2.2]PCP based CPL emitters in recent years, successfully used this strategy to design potent CPL emitters with exceptional g_{lum} values of up to 2.3×10^{-2}.[26–31] Other groups also contributed significantly to this field of research by synthesizing [2.2]PCP derivatives that can undergo thermally activated delayed fluorescence (TADF) or show solvent induced CPL sign switching.[32,33]

The dissymmetry factor of luminescence, g_{lum}, can be predicted accurately by computational chemistry, making it a powerful tool in guiding the discovery of highly efficient CPL active materials.[34–43] Following our previous strategy,[35] we computationally screened for potential CPL emitters and identified [2.2]fluorenonophane **1** as an interesting lead structure. **1** was synthesized first in 2021 by Wu *et al.*[44] and was never investigated for its chiroptical properties. We herein report that the readily accessible **1** has a remarkably high g_{lum} value, demonstrating the power of a synergistic approach to CPL materials.

The synthesis of the target compound **(R_p)-/(S_p)-1** is based on previous work by Wu *et al.* (Scheme 1).[44] The synthesis and optical resolution of the enantiopure starting material **(R_p)-/(S_p)-2** were performed according to the established protocol of

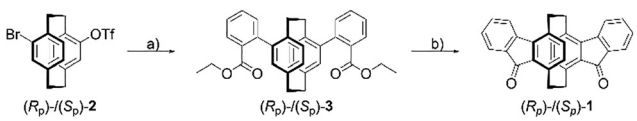

Scheme 1 Synthesis of **(R_p)-/(S_p)-1**. Reagents and conditions: (a) ethyl 2-(4,4,5,5-tetramethyl-1,3,2-dioxaborolan-2-yl)benzoate (3.00 eq.), SPHOS (20 mol%), $Pd(PPh_3)_4$ (20 mol%), tetrabutylammonium bromide (2.00 eq.), K_2CO_3 (6.00 eq.), xylene (isomeric mixture)/EtOH/H_2O (2 : 1 : 1 v/v), 120 °C, and 18 h, 77%; (b) polyphosphoric acid, 120 °C, 18 h, and 47%.

[a] Institut für Organische Chemie, Universität Tübingen, Auf der Morgenstelle 18, Tübingen 72076, Germany. E-mail: holger.bettinger@uni-tuebingen.de
[b] Institut für Physikalische und Theoretische Chemie, Universität Tübingen, Auf der Morgenstelle 18, Tübingen 72076, Germany. E-mail: marcus.scheele@uni-tuebingen.de
[c] Institut für Anorganische Chemie, Universität Tübingen, Auf der Morgenstelle 18, Tübingen 72076, Germany

Morisaki *et al.*, starting from the commercially available pseudo-*meta*-dibromo[2.2]paracyclophane.[26] **(R_p)-** and **(S_p)-2** were obtained with yields of 26% and 19%, respectively, and an ee ≥ 99.9% (estimated by HPLC analysis of the diastereomeric camphanic ester intermediates, Fig. S7, SI). The enantiopure **(R_p)-/(S_p)-2** was then transformed into **(R_p)-/(S_p)-3** *via* Suzuki cross coupling with a yield of 77%. In contrast to Wu *et al.*, we utilized the commercially available ethyl 2-(4,4,5,5-tetramethyl-1,3,2-dioxaborolan-2-yl)benzoate instead of ethyl-2-(5,5-dimethyl-1,3,2-dioxaborinan-2-yl)benzoate as the boronic acid component in the Suzuki cross coupling. In the last step, **(R_p)-/(S_p)-3** was cyclized to the target molecule **(R_p)-/(S_p)-1** *via* an intramolecular Friedel–Crafts reaction, catalyzed by polyphosphoric acid, with a yield of 47%. The target molecule **(R_p)-/(S_p)-1** was obtained as a yellow solid with an overall yield of 36% (over the two steps) and was characterized by ^{1}H, ^{13}C, and correlated NMR, high-resolution mass spectrometry, single-crystal X-ray crystallography and by (chir)optical methods.

Single crystals of enantiopure **(R_p)-1** suitable for X-ray crystallography were obtained by slow evaporation of a solution of the compound in a mixture of *n*-hexane and dichloromethane at 5 °C. **(R_p)-1** crystallizes in the triclinic space group *P*1, in contrast to the racemic mixture of **1**, for which Wu *et al.* reported the monoclinic $P2_1/c$ space group.[44] The compound adopts a π-stacked packing in the crystal with a distance of 3.37 Å between the molecules, indicating pronounced π–π interactions in the solid state (Fig. 1).

Compound **(R_p)-/(S_p)-1** dissolved in CH_2Cl_2 appears as a yellow solution and exhibits green fluorescence. The corresponding absorption and emission spectra (Fig. 2a) resemble the shape of previously reported spectra in toluene by Wu *et al.*[44] The absorption spectrum shows four features with band maxima at 269 nm ($\varepsilon_{269\ nm}$ = 47.3 × 10^3 M^{-1} cm^{-1}), 317 nm ($\varepsilon_{317\ nm}$ = 6.9 × 10^3 M^{-1} cm^{-1}), 366 nm ($\varepsilon_{366\ nm}$ = 3.1 × 10^3 M^{-1} cm^{-1}) and 416 nm ($\varepsilon_{416\ nm}$ = 1.5 × 10^3 M^{-1} cm^{-1}). The emission spectrum shows a broad structureless band with a maximum at 544 nm and a Stokes shift of 5660 cm^{-1} (Fig. 1a). The emission band shape, accompanied by a large Stokes shift, is characteristic of paracyclophanes and points to intramolecular excimer formation.[45,46] This interpretation is also supported by the difference between the ground and excited state dipole moments of $\Delta\mu$ = 8.09 D (determined *via* the Lippert–Mataga method; Fig. S11, SI), which is indicative of at least partial charge transfer during excitation.[47,48] In CH_2Cl_2, the quantum yield was absolutely determined to be Φ_{PL}(**1**) = 4% and the measured monoexponential lifetime τ was 7.67 ns (Fig. S10, SI). The quantum yield can be increased to 7% by changing the solvent to DMF (Table S1, SI). The compound also features strong positive solvatochromism where the emission maximum can be tuned from 509 nm in *n*-hexane up to 584 nm in methanol (Fig. S9, SI).

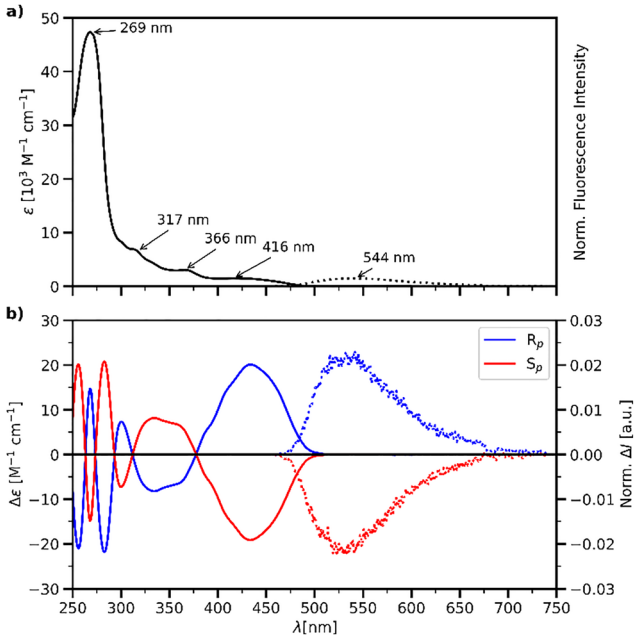

Fig. 2 (a) Absorption (solid line) and emission (dotted line, λ_{ex} = 405 nm) spectra of **rac-1** in CH_2Cl_2. (b) ECD (solid line) and CPL (dotted line, λ_{ex} = 405 nm) spectra of **(R_p)-/(S_p)-1** in CH_2Cl_2.

Enantiopure samples of **(R_p)-/(S_p)-1** were investigated for their chiroptical properties using electronic circular dichroism (ECD) and CPL spectroscopy (Fig. 2b). The ECD spectra of the enantiomers are perfectly mirrored and exhibit pronounced Cotton effects. The sign of circular dichroism is oscillating rapidly in the UV region between 250 and 280 nm, which probably originates from exciton coupling between the two fluorenone chromophores.[49] The dissymmetry factor of absorption, g_{abs}, derived from the lowest energy band at 433 nm of the ECD spectra is +1.3 × 10^{-2}/−1.3 × 10^{-2} for the R_p and S_p

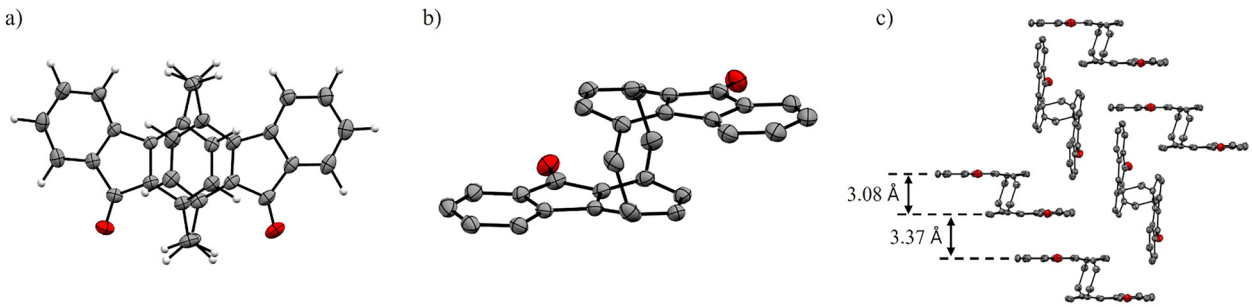

Fig. 1 Molecular structure of **(R_p)-1** in the solid state (CCDC: 2457695): (a) top view and (b) side view. (c) Packing of **(R_p)-1** in the solid state. Hydrogen atoms are omitted for clarity. Thermal ellipsoids are drawn at the 50% probability level.

enantiomers. The CPL spectra are characterized by one band with a maximum at around 530 nm corresponding to the emission maximum. The enantiomers exhibit strong CPL with dissymmetry factors (g_{lum}) of $+2.5 \times 10^{-2}/-2.6 \times 10^{-2}$ for the R_p and S_p enantiomers, respectively, which are unusually large for organic small molecules. In particular, when compared to other PCP based CPL emitters containing fused rings or carbonyl groups, **1** emerges as superior in terms of the g_{lum} value.[26,50–52] For example, it surpasses the coumarin system of Benedetti *et al.*, which displays a g_{lum} value of $\pm 5 \times 10^{-3}$ at a comparable quantum yield.[51] The chiral circularly polarized brightness $B_{CPL} = 1/2\varepsilon_\lambda \times \Phi_{lum} \times |g_{lum}|$ of **1** results in $B_{CPL} = 0.8$ M^{-1} cm^{-1} at an excitation wavelength of 405 nm. The g_{lum} value remains constant throughout the entire emission band (Fig. S15, SI), as expected for a single transition responsible for the emission. The dependence of g_{lum} on the solvent was also investigated by recording the CPL spectra in *n*-hexane, acetonitrile, chloroform, dimethylformamide, ethyl acetate and ethanol, but no significant difference in sign or magnitude of g_{lum} could be observed (Fig. S17–S22, SI). This indicates that the geometry of the emissive excited state does not depend significantly on the polarity of the solvent. It is also remarkable that the g_{lum}/g_{abs} ratio is greater than 1, which is in contradiction with the findings of Mori *et al.*, who reported an empirical correlation of $g_{lum} = 0.8 \times g_{abs}$ for π–π* transitions of small organic molecules.[53] Enhanced dissymmetry factors for the luminescence compared to the absorption can indicate intramolecular excimer formation, which is consistent with the previously discussed interpretation of the absorption and emission spectra.[54] In the literature, the amplification of g_{lum} through excimer formation has mainly been studied in systems containing pyrene as an excimer forming luminophore, where the g_{lum} values of the best performing representatives also exceeded 10^{-2}.[55–58] Hence, the reported [2.2]fluorenonophane provides a complementary system for the exploitation of excimer formation, enabling high g_{lum} values. Although the broad excimer emission band could be a drawback for actual application in devices, the reported emission spectrum of **1** is comparable to that of materials used to study circularly polarized electroluminescence.[32,59–62] Therefore **1**, with its simple structure but strong chiroptical response, has the potential to serve as a model system for application-oriented CPL research.

In order to gain more insight into the (chir)optical properties of **1**, the compound was studied computationally using TD-DFT (for more details, see the SI). The calculated absorption and ECD spectra obtained from single point TD-MN15/def2-TZVP (SMD: CH_2Cl_2) calculations are in good agreement with the measured ones (Fig. S23 and S24, SI).[63–65] The lowest energy transition from S_0 to S_1 is computed to be at 416 nm with a small oscillator strength (f = 0.0306). Hence, the observed absorption band with λ_{max} = 416 nm can be assigned to the $S_0 \rightarrow S_1$ transition, as it is in perfect agreement with the computed value. NTO analysis reveals that the nature of the $S_0 \rightarrow S_1$ transition is dominated by ππ* character (occupation = 0.85), where the π- and π*-orbitals are both delocalized over the whole molecule (Fig. S25, SI).

The parameters characterizing the emission properties were obtained by optimizing the emitting S_1 state at the TD-MN15/def2-TZVP level of theory. The calculated emission maximum of $\lambda_{Em.,calcd.}$ = 501 nm agrees reasonably well with the experimentally observed emission maximum of $\lambda_{Em.,max.}$ = 544 nm in dichloromethane. Also, the predicted $g_{lum,calcd.}$ value of 2.1×10^{-2} calculated from the electric ($\vec{\mu}$) and magnetic ($\vec{m}$) transition dipole moments reproduce the observed g_{lum} value of $+2.5 \times 10^{-2}/-2.6 \times 10^{-2}$ well. As g_{lum} is proportional to $\cos(\theta_{\mu,m})$ ($\theta_{\mu,m}$ is the angle between $\vec{\mu}$ and $\vec{m}$), the almost perfectly antiparallel alignment between the electric and magnetic transition dipole moment vectors $\vec{\mu}$ and $\vec{m}$ ($\theta_{\mu,m} = 178.4°$) is highly favorable and gives rise to the observed high g_{lum} value.[19] According to the calculations, only the HOMO→LUMO transition is responsible for the $S_1 \rightarrow S_0$ transition, which therefore possesses pure ππ* character (Fig. 3). While the LUMO (representing the emissive orbital in this context) is delocalized over the whole molecule with a significant transannular overlap between the two π-systems, the HOMO is localized on the central [2.2]paracyclophane unit with no transannular overlap between the π-systems. This supports the previously proposed interpretation of the spectroscopic data that the emissive state

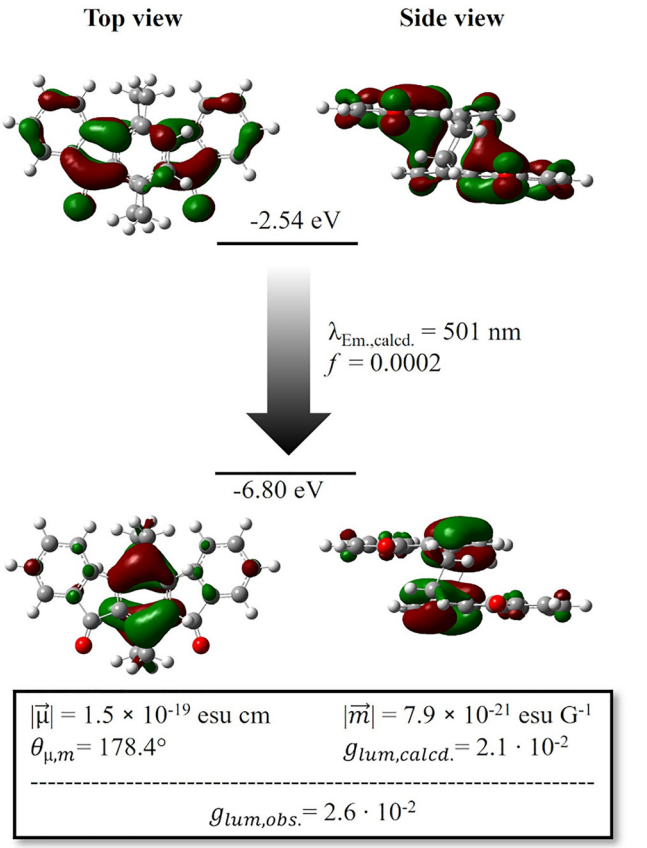

Fig. 3 Frontier molecular orbitals (visualized at an isovalue of 0.03) in the S_1 state, representing the $S_1 \rightarrow S_0$ transition with the computed values of the electronic transition properties in the S_1 state at the TD-MN15/def2-TZVP level of theory. f is the oscillator strength, $\vec{\mu}$ and $\vec{m}$ are the electric and magnetic transition dipole moments, respectively, and $\theta_{\mu,m}$ is the angle between $\vec{\mu}$ and $\vec{m}$.

exhibits excimer character and that the electronic transition features partial charge transfer.

In summary, we report the first enantiopure synthesis and chiroptical investigations of (**R_p**)-/(**S_p**)-**1**. Despite its simple structure, enantiopure samples of (**R_p**)-/(**S_p**)-**1** exhibit a strong chiral response in ECD and CPL spectroscopy, with high dissymmetry factors of $g_{abs} = \pm 1.3 \times 10^{-2}$ and $g_{lum} = +2.5 \times 10^{-2}/-2.6 \times 10^{-2}$. The enhanced dissymmetry factor for luminescence compared to absorption is probably attributed to intramolecular excimer formation. The chiroptical properties were accurately reproduced by TD-DFT calculations, highlighting the potential of computational chemistry in guiding the discovery of highly efficient CPL-active materials.

We gratefully acknowledge financial support from the Volkswagen Foundation under project 0072510-00. The computations were performed on bwForCluster JUSTUS2. The authors acknowledge support from the state of Baden-Württemberg through bwHPC and the German Research Foundation (DFG) through grant no. INST 40/575-1 FUGG (JUSTUS 2 cluster) for computational facilities.

Author contributions

A. Loleit: synthesis, analytics, computations, spectroscopy measurements (absorption and ECD), visualization, writing – original draft. L. Eckhardt: spectroscopy measurements (absorption, emission and CPL), visualization, writing – review & editing. M. Ströbele: X-ray crystallography. J. L. Hiller: construction of the CPL spectrometer setup. M. Scheele: conceptualization, funding acquisition, project administration, resources, writing – review & editing, supervision. H. F. Bettinger: conceptualization, funding acquisition, project administration, resources, writing – review & editing, supervision.

Conflicts of interest

There are no conflicts to declare.

Data availability

The data supporting this article have been included as part of the supplementary information (SI). Supplementary information is available. See DOI: https://doi.org/10.1039/d6cp00273k.

CCDC 2457695 ((**R_p**)-**1**) contains the supplementary crystallographic data for this paper.[66]

Notes and references

1 D.-Y. Kim, *J. Korean Phys. Soc.*, 2006, **49**, 505–508.
2 M. Schadt, *Annu. Rev. Mater. Sci.*, 1997, **27**, 305–379.
3 J. Harrold, A. M. S. Jacobs, G. Woodgate and D. Ezra, *Opt. Express*, 2010, **18**, 27079–27094.
4 F. Song, G. Wei, X. Jiang, F. Li, C. Zhu and Y. Cheng, *Chem. Commun.*, 2013, **49**, 5772–5774.
5 Y. Yang, R. C. Da Costa, M. J. Fuchter and A. J. Campbell, *Nat. Photonics*, 2013, **7**, 634–638.
6 Y. Imai, Y. Nakano, T. Kawai and J. Yuasa, *Angew. Chem., Int. Ed.*, 2018, **57**, 8973–8978.
7 J. F. Sherson, H. Krauter, R. K. Olsson, B. Julsgaard, K. Hammerer, I. Cirac and E. S. Polzik, *Nature*, 2006, **443**, 557–560.
8 C. Wagenknecht, C. M. Li, A. Reingruber, X. H. Bao, A. Goebel, Y. A. Chen, Q. Zhang, K. Chen and J. W. Pan, *Nat. Photonics*, 2010, **4**, 549–552.
9 H. Zheng, W. Li, W. Li, X. Wang, Z. Tang, S. Xiao-An Zhang, Y. Xu, H. Z. Zheng, W. R. Li, Y. Xu, W. Li, X. J. Wang, S. X.-A. Zhang and Z. Y. Tang, *Adv. Mater.*, 2018, **30**, 1705948.
10 J. P. Riehl and F. S. Richardson, *Chem. Rev.*, 1986, **86**, 1–16.
11 E. M. Sánchez-Carnerero, A. R. Agarrabeitia, F. Moreno, B. L. Maroto, G. Muller, M. J. Ortiz and S. De La Moya, *Chem. – Eur. J.*, 2015, **21**, 13488–13500.
12 Y. Zhang, S. Yu, B. Han, Y. Zhou, X. Zhang, X. Gao and Z. Tang, *Matter*, 2022, **5**, 837–875.
13 T. Zhang, Y. Zhang, Z. He, T. Yang, X. Hu, T. Zhu, Y. Zhang, Y. Tang and J. Jiao, *Chem. – Asian J.*, 2024, **19**, e202400049.
14 P. Izquierdo-García, J. M. Fernández-García, S. Medina Rivero, M. Šámal, J. Rybáček, L. Bednárová, S. Ramírez-Barroso, F. J. Ramírez, R. Rodríguez, J. Perles, D. García-Fresnadillo, J. Crassous, J. Casado, I. G. Stará and N. Martín, *J. Am. Chem. Soc.*, 2023, **145**, 11599–11610.
15 F. Saal, V. Brancaccio, K. Radacki, H. Braunschweig and P. Ravat, *Angew. Chem., Int. Ed.*, 2025, **64**, e202508779.
16 Q. Zhou, W. Yuan, Y. Li, Y. Han, L. Bao, W. Fan, L. Jiao, Y. Zhao, Y. Ni, Y. Zou, H. B. Yang and J. Wu, *Angew. Chem., Int. Ed.*, 2025, **64**, e202417749.
17 Y. Morisaki, M. Gon, T. Sasamori, N. Tokitoh and Y. Chujo, *J. Am. Chem. Soc.*, 2014, **136**, 3350–3353.
18 S. Sato, A. Yoshii, S. Takahashi, S. Furumi, M. Takeuchi and H. Isobe, *Proc. Natl. Acad. Sci. U. S. A.*, 2017, **114**, 13097–13101.
19 Y. Nagata and T. Mori, *Front. Chem.*, 2020, **8**, 535258.
20 I. Majerz and T. Dziembowska, *J. Phys. Chem. A*, 2016, **120**, 8138–8147.
21 D. J. Cram, N. L. Allinger and H. Steinberg, *J. Am. Chem. Soc.*, 1954, **76**, 6132–6141.
22 J. M. Teng, D. W. Zhang and C. F. Chen, *ChemPhotoChem*, 2022, **6**, e202100228.
23 K. I. Sugiura, *Front. Chem.*, 2020, **8**, 550015.
24 S. Felder, M. L. Delcourt, D. Contant, R. Rodríguez, L. Favereau, J. Crassous, L. Micouin and E. Benedetti, *J. Mater. Chem. C*, 2023, **11**, 2053–2062.
25 J.-F. Chen, Q.-X. Gao, H. Yao, B. Shi, Y.-M. Zhang, T.-B. Wei and Q. Lin, *Chem. Commun.*, 2024, **60**, 6728–6740.
26 M. Tsuchiya, H. Maeda, R. Inoue, Y. Morisaki and R. Li, *Chem. Commun.*, 2021, **57**, 9256–9259.
27 A. Yanagawa, R. Inoue, Y. Morisaki and R. Li, *Chem. Commun.*, 2024, **60**, 1468–1471.
28 K. Matsumura, R. Inoue and Y. Morisaki, *Adv. Funct. Mater.*, 2024, **34**, 2310566.
29 Y. Morisaki, K. Inoshita and Y. Chujo, *Chem. – Eur. J.*, 2014, **20**, 8386–8390.
30 A. Morisaki, R. Inoue and Y. Morisaki, *Chem. – Eur. J.*, 2023, **29**, e202203533.

31 M. Gon, Y. Morisaki, R. Sawada and Y. Chujo, *Chem. – Eur. J.*, 2016, **22**, 2291–2298.
32 N. Sharma, E. Spuling, C. M. Mattern, W. Li, O. Fuhr, Y. Tsuchiya, C. Adachi, S. Bräse, I. D. W. Samuel and E. Zysman-Colman, *Chem. Sci.*, 2019, **10**, 6689–6696.
33 M. Y. Zhang, X. Liang, D. N. Ni, D. H. Liu, Q. Peng and C. H. Zhao, *Org. Lett.*, 2021, **23**, 2–7.
34 M. R. Rapp, W. Leis, F. Zinna, L. Di Bari, T. Arnold, B. Speiser, M. Seitz and H. F. Bettinger, *Chem. – Eur. J.*, 2022, **28**, e2021041.
35 M. R. Rapp, P. Ziemann, F. Zinna, L. Di Bari and H. F. Bettinger, *J. Mater. Chem. C*, 2023, **11**, 15767.
36 F. Zinna, T. Bruhn, C. A. Guido, J. Ahrens, M. Bröring, L. Di Bari and G. Pescitelli, *Chem. – Eur. J.*, 2016, **22**, 16089–16098.
37 H. R. McAlexander and T. D. Crawford, *J. Chem. Phys.*, 2015, **142**, 154101.
38 B. Pritchard and J. Autschbach, *ChemPhysChem*, 2010, **11**, 2409–2415.
39 J. Schlessinger and A. Warshel, *Chem. Phys. Lett.*, 1974, **28**, 380–383.
40 H. Kubo, T. Hirose, T. Nakashima, T. Kawai, J. Y. Hasegawa and K. Matsuda, *J. Phys. Chem. Lett.*, 2021, **12**, 686–695.
41 M. Pecul and K. Ruud, *Phys. Chem. Chem. Phys.*, 2010, **13**, 643–650.
42 G. Longhi, E. Castiglioni, J. Koshoubu, G. Mazzeo and S. Abbate, *Chirality*, 2016, **28**, 696–707.
43 C. A. Guido, F. Zinna and G. Pescitelli, *J. Mater. Chem. C*, 2023, **11**, 10474–10482.
44 C. S. Wang, Y. C. Wei, M. L. Pan, C. H. Wu, P. T. Chou and Y. T. Wu, *Chem. – Eur. J.*, 2021, **27**, 8678–8683.
45 T. Förster, *Angew. Chem., Int. Ed. Engl.*, 1969, **8**, 333–343.
46 G. C. Bazan, W. J. Oldham, R. J. Lachicotte, S. Tretiak, V. Chernyak and S. Mukamel, *J. Am. Chem. Soc.*, 1998, **120**, 9188–9204.
47 N. Mataga, Y. Kaifu and M. Koizumi, *Bull. Chem. Soc. Jpn.*, 1956, **29**, 465–470.
48 E. Lippert, *Ber. Bunsenges. Phys. Chem.*, 1957, **61**, 962–975.
49 N. Berova, L. Di Bari and G. Pescitelli, *Chem. Soc. Rev.*, 2007, **36**, 914–931.
50 S. Felder, M. L. Delcourt, M. H. E. Bousquet, D. Jacquemin, R. Rodríguez, L. Favereau, J. Crassous, L. Micouin and E. Benedetti, *J. Org. Chem.*, 2022, **87**, 147–158.
51 M. L. Delcourt, C. Reynaud, S. Turcaud, L. Favereau, J. Crassous, L. Micouin and E. Benedetti, *J. Org. Chem.*, 2019, **84**, 888–899.
52 C. H. Chen and W. H. Zheng, *Org. Lett.*, 2021, **23**, 5554–5558.
53 H. Tanaka, Y. Inoue and T. Mori, *ChemPhotoChem*, 2018, **2**, 386–402.
54 F. Zinna, E. Brun, A. Homberg and J. Lacour, *Circularly polarized luminescence of isolated small organic molecules*, ed. T. Mori, Springer, Singapore, 2020, pp. 273–292.
55 N. Hara, M. Shizuma, T. Harada and Y. Imai, *RSC Adv.*, 2020, **10**, 11335–11338.
56 V. Zullo, A. Iuliano, G. Pescitelli and F. Zinna, *Chem. – Eur. J.*, 2022, **28**, e202104226.
57 H. Shigemitsu, K. Kawakami, Y. Nagata, R. Kajiwara, S. Yamada, T. Mori and T. Kida, *Angew. Chem., Int. Ed.*, 2022, **61**, e202114700.
58 K. Takaishi, S. Murakami, F. Yoshinami, T. Ema, K. Takaishi, S. Murakami, F. Yoshinami and T. Ema, *Angew. Chem., Int. Ed.*, 2022, **61**, e202204609.
59 R. Chowdhury, M. D. Preuss, H. H. Cho, J. J. P. Thompson, S. Sen, T. K. Baikie, P. Ghosh, Y. Boeije, X. W. Chua, K. W. Chang, E. Guo, J. van der Tol, B. W. L. van den Bersselaar, A. Taddeucci, N. Daub, D. M. Dekker, S. T. Keene, G. Vantomme, B. Ehrler, S. C. J. Meskers, A. Rao, B. Monserrat, E. W. Meijer and R. H. Friend, *Science*, 2025, **387**, 1175–1181.
60 F. Furlan, M. Šámal, J. Rybáček, A. Taddeucci, M. Di Girolamo, D. Nodari, G. Siligardi, J. Wade, B. Yan, I. G. Stará, N. Gasparini and M. J. Fuchter, *Nat. Photonics*, 2025, **19**, 1361–1366.
61 Y. Xu, H. Hafeez, J. Seibert, S. Wu, J. S. O. Ortiz, J. Crassous, S. Bräse, I. D. W. Samuel and E. Zysman-Colman, *Adv. Funct. Mater.*, 2024, **34**, 2402036.
62 M. Gong, L. Yuan, Y. X. Zheng and W. H. Zheng, *Adv. Funct. Mater.*, 2024, **34**, 2314205.
63 H. S. Yu, X. He, S. L. Li and D. G. Truhlar, *Chem. Sci.*, 2016, **7**, 5032–5051.
64 F. Weigend and R. Ahlrichs, *Phys. Chem. Chem. Phys.*, 2005, **7**, 3297–3305.
65 A. V. Marenich, C. J. Cramer and D. G. Truhlar, *J. Phys. Chem. B*, 2009, **113**, 6378–6396.
66 CCDC 2457695: Experimental Crystal Structure Determination, 2026, DOI: 10.5517/ccdc.csd.cc2nhfh3.